JACS
JOURNAL OF THE AMERICAN CHEMICAL SOCIETY
Communication
pubs.acs.org/JACS

# Tunable and Switchable Dielectric Constant in an Amphidynamic Crystal

Wen Zhang,*[,†] Heng-Yun Ye,[†] Robert Graf,[‡] Hans W. Spiess,[‡] Ye-Feng Yao,*[,§] Run-Qiang Zhu,[†] and Ren-Gen Xiong[†]

[†]Ordered Matter Science Research Center, Southeast University, Nanjing 211189, P.R. China

[‡]Max-Planck-Institute for Polymer Research, Ackermannweg 10, 55128 Mainz, Germany

[§]Department of Physics & Shanghai Key Laboratory of Magnetic Resonance, East China Normal University, North Zhongshan Road 3663, Shanghai 200062, P.R. China

Supporting Information

**ABSTRACT:** The inclusion compound $[(CH_3)_2NH_2]_2[KCo(CN)_6]$ exhibits a marked temperature-dependent dielectric constant and can be considered as a model of tunable and switchable dielectric materials. Crystal structure and solid-state NMR studies reveal a switchable property between low and high dielectric states around 245 K. This originates from an order−disorder phase transition of the system, changing the dynamics of the polar dimethylammonium (DMA) cation. Furthermore, the tuning of the dielectric constant at temperatures below the phase transition point is related to increasing angular pretransitional fluctuations of the dipole moment of DMA.

Electrically polarizable materials exhibit rich dielectric, piezoelectric, pyroelectric, and ferroelectric properties and have widespread applications.[1] For example, dielectric materials are basic components of modern electrical and electronic devices. Each of these materials is characterized by a dielectric constant $\varepsilon$ ($\varepsilon = \varepsilon' - i\varepsilon''$, where $\varepsilon'$ and $\varepsilon''$ are the real and imaginary parts, respectively) that is related to microscopic polarizability of the material. The $\varepsilon'$ value of silicon nitride (∼7) is usually used as a boundary between high and low dielectric constant materials, both of which are of interest for different applications.[2]

For a compound containing polar molecules, dipolar reorientation can contribute significantly to the dielectric response. In some cases, motions of the dipoles can be switched on or off by external stimuli such as temperature. These responsive materials, designated as switchable dielectrics, can undergo a transition between high and low dielectric states at a phase transition temperature ($T_c$). Basically, the switching of the dielectric constant at the $T_c$ is due to motional changes of polar molecules or ions between "rotating or hopping" (melt-like) and orientationally ordered (frozen) states, which correspond to a high-temperature phase (HTP) and low-temperature phase (LTP), respectively. By considering only the contribution of the dipolar reorientation of an ideal single-phase system (nearly independent particle system), and defining a net dielectric constant $\varepsilon_d' = (\varepsilon' - \varepsilon'_{LTP})$, which equals $C/T$ ($C$ is a constant and $T$ the temperature) in the HTP and zero in the LTP, we can clearly describe the switching property (model A; for a detailed discussion see the Supporting Information). Switchable dielectrics have a magnetic counterpart, i.e., spin crossover compounds, for which spin pairing and unpairing result in a transition between low- and high-spin states.[3]

Switchable dielectrics can be found in a special type of crystalline compounds, termed amphidynamic crystals by Garcia-Garibay to describe an assembly of periodically arranged molecules in the solid state that contain both rigid and mobile (e.g., rotational) components.[4−6] Tuning and switching motions of the polar rotators in amphidynamic crystals naturally correlate with dielectric, ferroelectric, and electrooptic functions which have been long envisioned and pursued.[7−9] Perovskite-type metal−organic frameworks (MOFs) are highly suited to the generation of amphidynamic crystals, because their structures can be finely tuned by the combination of well-matched rigid cavities and mobile guest molecules, or ions, as carriers of electric dipole moments. Reports of switchable dielectric properties of such MOFs, however, have been scarce. This is due to a lack of knowledge of the geometry of the motion of the polar molecules in different phases, and of the relationship between molecular dynamics and the tuning and switching properties.[8d] Here, we present the inclusion compound $[(CH_3)_2NH_2]_2[KCo(CN)_6]$ (**1**) as an example of well-designed MOF-based switchable dielectrics. Different molecular dynamics of the polar DMA guests were characterized below and above a structural phase transition point, which allow tuning and switching of the dielectric constant.

Compound **1** was crystallized from an aqueous solution of $K_3[Co(CN)_6]$ and $[(CH_3)_2NH_2]Cl$ salts, by slow evaporation at room temperature, as pale-yellow block crystals. A variable-temperature single-crystal X-ray diffraction (XRD) study of **1** was performed in the range 113−293 K. The structure at 293 K (HTP) belongs to the tetragonal space group $P4/mnc$, with $a = b = 8.290(1)$ Å and $c = 11.621(3)$ Å. The most striking structural feature is the double perovskite structure, known as cyano-elpasolite $A_2[B'B''(CN)_6]$ (A = monovalent cation, B′(I) = monovalent metal, and B″(III) = trivalent metal), in which the cationic A guest is located in the cage formed by B′−NC−B″.[10] In **1**, the anionic cage is formed by Co−C≡N−K units (Figure 1a). The metal−cyanide bond is strong and covalent in the fragment $Co(CN)_6$ (Co−C ≈ 1.9 Å) and much weaker and ionic

**Received:** November 12, 2012
**Published:** March 21, 2013

ACS Publications © 2013 American Chemical Society



dx.doi.org/10.1021/ja3110335 | J. Am. Chem. Soc. 2013, 135, 5230−5233

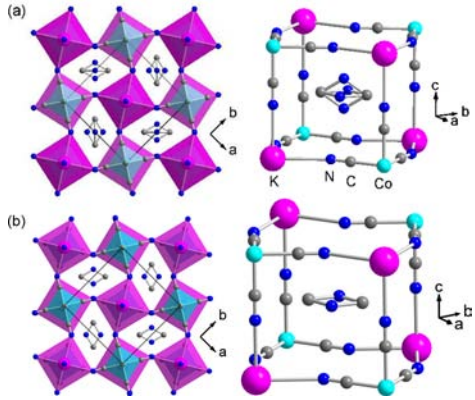


**Figure 1.** Packing diagrams viewed along the *c* axis and cage structures of **1** at (a) 293 K (HTP) and (b) 113 K (LTP). The DMA cation is disordered over four sites at 293 K, shown as an octahedron, and more ordered over two sites at 113 K, shown as a rhombus. H atoms are omitted for clarity.

in the fragment $K(NC)_6$ (K–N ≈ 3.0 Å). The $K^+$ ion adopts an octahedral coordination geometry compressed along the *c* axis, with equatorial K–N = 2.955(3) Å and apical K–N = 2.780(4) Å. Each $[K_4Co_4(CN)_{12}]$ cage accommodates a DMA cation that displays orientational disorder over four sites. The site occupancies of the N atom are 0.30, 0.20, 0.30, and 0.20. It should be noted that the anionic cage is not a cube or a regular hexahedron, but a concave decahedron that is tuned by the shape of the DMA guest as a template. The crystal structure at 113 K (LTP) still adopts the same space group with similar cell parameters of $a = b = 8.242(6)$ Å and $c = 11.584(10)$ Å. However, the DMA cation shows disorder only over two sites, with equal occupancies in the *ab* plane (Figure 1b). The disorder over the other two sites disappears in the crystal lattice.

Compared with molecular rotors, **1** shows characteristics of a MOF-based rotor or compass.[4−6] The $[K_4Co_4(CN)_{12}]$ cage provides the stator while the DMA acts as the polar rotator, and both parts are connected by a virtual axis along the [110] or [$\bar{1}$10] direction (HTP) (Figure 2). This makes **1** different from covalently bonded molecular rotors. The ratio of the components of the dipole moment along the [001] and [110] directions is found to be 2:1. The dynamics of the rotators will be discussed below.

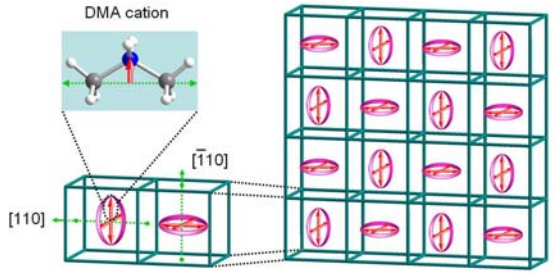


**Figure 2.** Array of dipole moments (red arrows) in the crystal lattice of the HTP. Here we assume that the negative charge of the cage is located at the center of the octahedron of the DMA cation. Thus, the dipole moment produced by the separate positive–negative point charges is superimposed on the permanent dipole moment of the polar DMA backbone, in the same direction. The net dipole moment points from the center of the octahedron to the N atom of the DMA cation. In the cage, the dipole moment shows four perpendicular directions (from the crystallographic viewpoint) confined in a plane shown as a purple circle. In the crystal lattice, the planes have two orientations, [110] and [$\bar{1}$10], respectively.

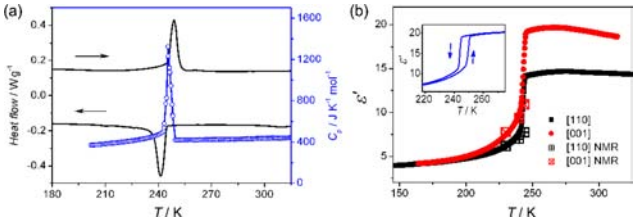


**Figure 3.** Thermal and dielectric characterizations of the structural phase transition in **1**: (a) DSC and $C_p$ plots. (b) Temperature-dependent dielectric constant of **1** along the [001] and [110] directions at 1000 kHz upon cooling. Square symbols represent fitting points from the NMR results. Inset: thermal hysteresis at 1000 kHz.

Differential scanning calorimetry (DSC) and specific heat ($C_p$) measurements in the temperature range 190–310 K (Figure 3a) indicate a structural phase transition of **1** at 245 K, consistent with the X-ray analysis. The sharp peaks and the thermal hysteresis in the DSC curves and the $\lambda$-shaped peak in the $C_p$ curve show the characteristics of a first-order phase transition. The entropy increase, $\Delta S$, around $T_c$ is 13.0 J $K^{-1}$ $mol^{-1}$. An estimate of the number of molecular orientations from the calorimetric data yields $N$ = 4.8, based on the Boltzmann equation, $\Delta S = R\ln(N)$, where $R$ is the gas constant and $N$ is the ratio of the numbers of respective geometrically distinguishable orientations in both phases. This indicates that the DMA cations are much more disordered in the HTP than in the LTP, consistent with the single-crystal XRD data discussed above.

The dielectric constant of crystal samples of **1** cut perpendicular to the (001) and (110) planes was measured (Figure 3b and Supporting Information). We note that $\varepsilon'$ is dominated by $\varepsilon_d'$, and that the dipole moment of the DMA cation is directed along the bisector of the H–N–H bond angle, along a $C_2$ symmetry axis of the ion. With decreasing temperature, $\varepsilon'$ displays a relatively sharp transition about 245 K, consistent with the results of XRD and thermal analysis discussed above. The real part $\varepsilon'$ of the complex dielectric constant along the [001] direction is as high as 19 at 250 K in the HTP, but only around 4 at 150 K in the LTP, at 1000 kHz, corresponding to the high- and low-dielectric states, respectively. The value of $\varepsilon'$ in the high-dielectric state is approximately quadruple that in the low-dielectric state. In the frequency range 1–1000 kHz, $\varepsilon'$ is nearly frequency-independent, indicating that the orientations of the dipole moments can easily follow the oscillating electric field at the measured frequencies. Dielectric anisotropy of **1** is also confirmed. In the HTP, the values of the $\varepsilon'$ are about 19 and 14 along the [001] and [110] directions, respectively. The anisotropy of the dielectric constant, however, is lower than expected from the ratio of the components of the dipole moments noted above. Upon cooling and heating, the dielectric constants of **1** exhibit a thermal hysteresis of about 8 K (Figure 3b), consistent with a first-order phase transition.

Moreover, the dielectric constant $\varepsilon'$ of **1** exhibits a marked increase at temperatures below the $T_c$ and a decrease from the maximum value at temperatures above the $T_c$. As shown in the Supporting Information, this behavior can be interpreted as a pretransitional effect due to fluctuations characteristic of a weak second-order phase transition at the $T_c$, which hints at weak cooperativity of the dipoles. However, there is no ferroelectric ordering in **1** because a temperature-dependent second harmonic generation measurement of **1** shows no signals of a


dx.doi.org/10.1021/ja3110335 | J. Am. Chem. Soc. 2013, 135, 5230–5233

noncentrosymmetric structure. This is quite different from a recently reported family of MOFs, $[(CH_3)_2NH_2][M^{II}(HCOO)_3]$ (M = Mn, Fe, Co, Ni, Zn), in which the disorder−order transition of the DMA cation is the origin of ferroelectric ordering.[9a,b] In these compounds, strong hydrogen bonds between the cationic guest and the metal−formate host are responsible for the paraelectric-to-ferroelectric phase transitions.

In order to quantify these observations, the molecular dynamics of the DMA cations in **1** were investigated by wide-line $^2$H NMR spectroscopy (Figure 4).[11,12] This method can

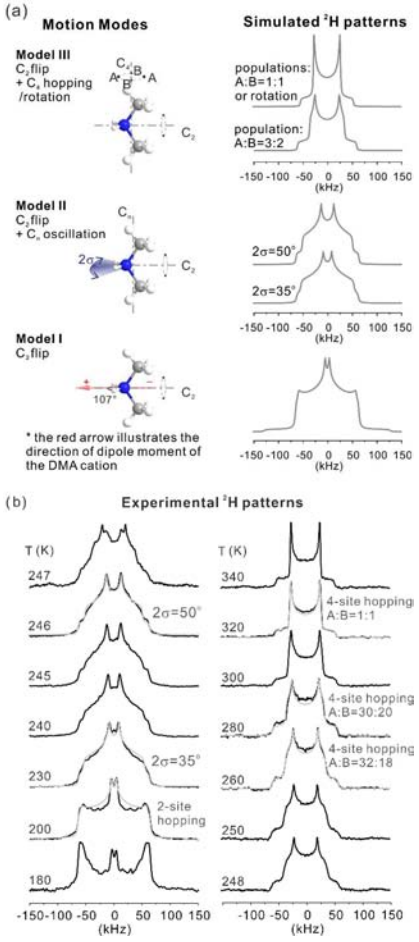


**Figure 4.** Simulated and experimental $^2$H NMR spectra of **2** at different temperatures. (a) Illustration of three motion modes of DMA in the cage, and simulated $^2$H patterns based on the motion modes. (b) Variable-temperature solid-state $^2$H patterns of **2** measured in the temperature range 180−340 K (black line). The simulated spectra are shown as gray lines.

determine the geometries of the rotational motions of the trapped molecules,[13] in addition to the time scale, by virtue of the nuclear quadrupole interaction. To this end, the amino protons of the DMA cation were selectively deuterated to yield $[(CH_3)_2ND_2]_2[KCo(CN)_6]$ (**2**). The experimental $^2$H NMR spectra of **2** at different temperatures display marked changes over large temperature ranges, both below and above the $T_c$ (Figure 4b). At none of the temperatures was the characteristic Pake pattern of $^2$H NMR spectra spanning more than 250 kHz in width, indicating an absence of motion, observed.[11] Moreover, it should be noted that the line shapes indicate rotational molecular motions with rates exceeding the width of the $^2$H spectra in the rigid case. Figure 4a shows three motional modes of DMA and the corresponding simulated line shapes. It is evident that the experimental spectra at 180 and 200 K can be described by model I, and those in the range 230−250 K by model II; at temperatures above 260 K, well above the phase transition, model III applies. Thus, the different $^2$H NMR line shapes in Figure 4b indicate that the DMA cations in the cage exhibit different reorientation processes at different temperatures. By simulating the patterns, we have obtained detailed information on the reorientation processes and its relationship to the dielectric behavior (see Supporting Information):

- At low temperatures, the $^2$H NMR line shape indicates that the DMA cations perform 180° flips about the axis of the electric dipole ($C_2$ axis, model I). This symmetry-conserving mode does not change the orientation of the dipole moment and is thus dielectrically inactive.
- When approaching the phase transition at 246 K, the two singularities at the top of the patterns separate gradually, as shown in Figure 4b. These spectral changes are attributed to in-plane oscillatory fluctuations around the long axis of the molecule ($C_n$) in addition to the 180° flip (model II). The oscillation amplitude determines the distance between the two singularities.[14] These oscillations change the orientation of the dipole moment and are therefore dielectrically active. As shown in the Supporting Information, the gradual increase in their amplitude can be directly related to the increasing dielectric relaxation strength. In order to achieve quantitative agreement between the angular fluctuations as determined by $^2$H NMR spectroscopy and dielectric data, as shown in Figure 3b, the lattice contribution to $\varepsilon'$ has to be taken into account.
- At temperatures above 260 K, well above the phase transition, the $^2$H NMR pattern further narrows and reaches the characteristic motionally averaged Pake pattern at 320 K. As shown in the Supporting Information, the unique axis of the motionally averaged quadrupole tensor is along the $C_n$ axis of DMA, and the rotation geometry is at least 4-fold. Inspired by the symmetry of the cage, we simulated the line shape by approximate $C_4$-hopping, allowing unequal populations of $C_2$ symmetry at temperatures between the phase transition and 320 K. In addition, the 180° flips about the $C_2$ axis also remain activated at these temperatures too (model III).

We note that models I and III have been used before to describe the motion of dimethylammonium halide in a solid.[12] The unequal populations of the four hopping sites, as indicated in the NMR patterns, are consistent with the XRD data discussed above, which indicate that in the HTP, the four sites of the DMA cation, represented as an octahedron, have different occupancies (see Supporting Information). Near the phase transition at 247 K, the $^2$H line shape exhibits features of both phases, most likely due to a slight temperature gradient typically present in NMR probes. This emphasizes the observation that the structural phase transition at the $T_c$ is of first order. The geometry of the motion of the DMA guests in the different phases was also probed by $^{13}$C NMR spectroscopy (Figure S12). Quantitative agreement between experimental and simulated line shapes is obtained with the models described above. This shows that the DMA ions rotate classically as a whole entity. Thus, the temperature-dependent motions of the DMA ions revealed by $^2$H NMR


dx.doi.org/10.1021/ja3110335 | J. Am. Chem. Soc. 2013, 135, 5230−5233

provide a deep understanding of the dielectric constant variation at the different temperatures in the two phases, as shown in Figure 3b, as well as of the pronounced pretransitional variation of $\varepsilon'$. Moreover, the temperature dependence of $\varepsilon'$ strongly deviates from the simple expectation (Figure S1). This indicates that other factors, such as interfacial polarization and the inorganic framework, also contribute to $\varepsilon'$. A quantitative analysis of this contribution is beyond the scope of this Communication. The gradual increase of the angular oscillations below the $T_c$, however, offers a way to tune $\varepsilon'$, and the phase transition itself allows switching the dielectric constant.

In conclusion, a MOF-based inclusion compound, $[(CH_3)_2NH_2]_2[KCo(CN)_6]$, was synthesized and characterized as a model compound of tunable and switchable dielectric materials. This compound shows a striking increase of the dielectric constant over a large temperature range, followed by a switch between low- and high-dielectric states at a phase transition around 245 K. Variable-temperature single-crystal XRD and solid-state NMR measurements disclose that the cationic DMA guest in the host cage exhibits pronounced pretransitional fluctuations similar to those found in second-order phase transitions. Moreover, the DMA drastically changes its motional behavior by undergoing an order−disorder-type structural phase transition. This generates a dielectric constant which is switchable at the $T_c$ and tunable over a significant range at temperatures below the $T_c$. Our findings indicate a new type of functional material with potential applications in molecular switches and electronic materials.[15] The scaling behavior of the pretransitional effects indicates a weak cooperativity of the motion of the DMA dipoles. Thus, the exploration of the mechanism of this tunable and switchable dielectric is closely related to ferroelectrics and artificial molecular rotors.[16,17]

## ■ ASSOCIATED CONTENT

### Ⓢ Supporting Information

Experimental details, Figures S1−S15, and CIF file. This material is available free of charge via the Internet at http://pubs.acs.org.

## ■ AUTHOR INFORMATION


### Corresponding Author

zhangwen@seu.edu.cn; yfyao@phy.ecnu.edu.cn


### Notes

The authors declare no competing financial interest.

## ■ ACKNOWLEDGMENTS

We acknowledge support from NSFC (grants 21071030, 21225102, 20804016, 21174039, and 90922005) and MEC (grant NCET-10-0333), and illuminating discussions with Prof. Ulrich Haeberlen (Heidelberg) and Prof. George Floudas (Ioannina). The anonymous reviewers are greatly appreciated for their valuable comments, which helped us to improve the paper.

## ■ REFERENCES


(1) (a) Ye, Z. G., Ed. *Handbook of advanced dielectric, piezoelectric and ferroelectric materials: Synthesis, properties and applications*; Woodhead Publishing: Cambridge, U.K., 2008. (b) Lines, M. E.; Glass, A. M. *Principles and Applications of Ferroelectrics and Related Materials*; Oxford University Press: Oxford, U.K., 1991.

(2) (a) Simon, P.; Gogotsi, Y. *Nat. Mater.* **2008**, *7*, 845−854. (b) Kohl, P. A. *Annu. Rev. Chem. Biomol. Eng.* **2011**, *2*, 379−401.

(3) (a) Kahn, O. *Molecular Magnetism*; VCH Publishers: New York, 1993. (b) Gütlich, P.; Goodwin, H. A. *Top. Curr. Chem.* **2004**, 233−235. (c) Sato, O.; Tao, J.; Zhang, Y. Z. *Angew. Chem., Int. Ed.* **2007**, *46*, 2152−2187.

(4) (a) Kottas, G. S.; Clarke, L. I.; Horinek, D.; Michl, J. *Chem. Rev.* **2005**, *105*, 1281−1376. (b) Michl, J.; Sykes, E. C. H. *ACS Nano* **2009**, *3*, 1042−1048.

(5) (a) Garcia-Garibay, M. A. *Proc. Natl. Acad. Sci. U.S.A.* **2005**, *102*, 10771−10776. (b) Karlen, S. D.; Garcia-Garibay, M. A. *Top. Curr. Chem.* **2005**, *262*, 179−227. (c) Khuong, T.-A. V.; Nuñez, J. E.; Godinez, C. E.; Garcia-Garibay, M. A. *Acc. Chem. Res.* **2006**, *39*, 413−422. (d) Vogelsberg, C. S.; Garcia-Garibay, M. A. *Chem. Soc. Rev.* **2012**, *41*, 1892−1910.

(6) (a) Dominguez, Z.; Dang, H.; Strouse, M. J.; Garcia-Garibay, M. A. *J. Am. Chem. Soc.* **2001**, *124*, 7719−7727. (b) Dominguez, Z.; Dang, H.; Strouse, M. J.; Garcia-Garibay, M. A. *J. Am. Chem. Soc.* **2002**, *124*, 2398−2399. (c) Dominguez, Z.; Khuong, T.-A. V.; Dang, H.; Sanrame, C. N.; Nuñez, J. E.; Garcia-Garibay, M. A. *J. Am. Chem. Soc.* **2003**, *125*, 8827−8837. (d) Gould, S. L.; Tranchemontagne, D.; Yaghi, O. M.; Garcia-Garibay, M. A. *J. Am. Chem. Soc.* **2008**, *130*, 3246−3247. (e) Rodriguez-Molina, B.; Ochoa, E. M.; Farfán, N.; Santillan, R.; Garcia-Garibay, M. A. *J. Org. Chem.* **2009**, *74*, 8554−8565. (f) Karlen, S. D.; Reyes, H.; Taylor, R. E.; Khan, S. I.; Hawthorne, M. F.; Garcia-Garibay, M. A. *Proc. Natl. Acad. Sci. U.S.A.* **2010**, *107*, 14973−14977. (g) Rodríguez-Molina, B.; Farfán, N.; Romero, M.; Méndez-Stivalet, J. M.; Santillan, R.; Garcia-Garibay, M. A. *J. Am. Chem. Soc.* **2011**, *133*, 7280−7283. (h) Lemouchi, C.; Vogelsberg, C. S.; Zorina, L.; Simonov, S.; Batail, P.; Brown, S.; Garcia-Garibay, M. A. *J. Am. Chem. Soc.* **2011**, *133*, 6371−6379.

(7) (a) Akutagawa, T.; Koshinaka, H.; Sato, D.; Takeda, S.; Noro, S.; Takahashi, H.; Kumai, R.; Tokura, Y.; Nakamura, T. *Nat. Mater.* **2009**, *8*, 342−347. (b) de Jonge, J. J.; Ratner, M. A.; de Leeuw, S. W. *J. Phys. Chem. C* **2007**, *111*, 3770−3777. (c) Kobr, L.; Zhao, K.; Shen, Y.; Comotti, A.; Bracco, S.; Shoemaker, R. K.; Sozzani, P.; Clark, N. A.; Price, J. C.; Rogers, C. T.; Michl, J. *J. Am. Chem. Soc.* **2012**, *134*, 10122−10131.

(8) (a) Horansky, R. D.; Clarke, L. I.; Price, J. C.; Khuong, T.-A. V.; Jarowski, P. D.; Garcia-Garibay, M. A. *Phys. Rev. B* **2005**, *72*, 014302. (b) Horansky, R. D.; Clarke, L. I.; Winston, E. B.; Price, J. C.; Karlen, S. D.; Jarowski, P. D.; Santillan, R.; Garcia-Garibay, M. A. *Phys. Rev. B* **2006**, *74*, 054306. (c) Winston, E. B.; Lowell, P. J.; Vacek, J.; Chocholoušová, J.; Michl, J.; Price, J. C. *Phys. Chem. Chem. Phys.* **2008**, *10*, 5188−5191. (d) Zhang, W.; Cai, Y.; Xiong, R.-G.; Yoshikawa, H.; Awaga, K. *Angew. Chem., Int. Ed.* **2010**, *49*, 6608−6610. (e) Devautour-Vinot, S.; Maurin, G.; Serre, C.; Horcajada, P.; da Cunha, D. P.; Guillerm, V.; Costa, E. D.; Taulelle, F.; Martineau, C. *Chem. Mater.* **2012**, *24*, 2168−2177. (f) Pato-Doldán, B.; Sánchez-Andújar, M.; Gómez-Aguirre, L. C.; Yáñez-Vilar, S.; López-Beceiro, J.; Gracia-Fernández, C.; Haghighirad, A. A.; Ritter, F.; Castro-García, S.; Señarís-Rodríguez, M. A. *Phys. Chem. Chem. Phys.* **2012**, *14*, 8498−8501.

(9) (a) Jain, P.; Dalal, N. S.; Toby, B. H.; Kroto, H. W.; Cheetham, A. K. *J. Am. Chem. Soc.* **2008**, *130*, 10450−10451. (b) Jain, P.; Ramachandran, V.; Clark, R. J.; Zhou, H. D.; Toby, B. H.; Dalal, N. S.; Kroto, H. W.; Cheetham, A. K. *J. Am. Chem. Soc.* **2009**, *131*, 13625−13627. (c) Zhang, Y.; Zhang, W.; Li, S.-H.; Ye, Q.; Cai, H.-L.; Deng, F.; Xiong, R.-G.; Huang, S. D. *J. Am. Chem. Soc.* **2012**, *134*, 11044−11049.

(10) Swanson, B. I.; Ryan, R. R. *Inorg. Chem.* **1973**, *12*, 283−286.

(11) (a) Schmidt-Rohr, K.; Spiess, H. W. *Multidimensional Solid-State NMR and Polymers*; Academic Press: London, 1994. (b) Hansen, M. R.; Graf, R.; Spiess, H. W. *Acc. Chem. Res.* **2013**, DOI: 10.1021/ar300338b.

(12) Ratcliffe, C. I. *J. Phys. Chem.* **1990**, *94*, 152−157.

(13) Shenderovich, I. G.; Buntkowsky, G.; Schreiber, A.; Gedat, E.; Sharif, S.; Albrecht, J.; Golubev, N. S.; Findenegg, G. H.; Limbach, H. H. *J. Phys. Chem. B* **2003**, *107*, 11924−11939.

(14) Macho, V.; Brombacher, L.; Spiess, H. W. *Appl. Magn. Reson.* **2001**, *20*, 405−432.

(15) (a) Feringa, B. L., Ed. *Molecular Switches*; Wiley-VCH: Weinheim, Germany, 2001. (b) Balzani, V.; Credi, A.; Venturi, M. *Molecular devices and machines*; Wiley-VCH: Weinheim, 2008.

(16) Zhang, W.; Xiong, R.-G. *Chem. Rev.* **2012**, *112*, 1163−1195.

(17) Browne, W. R.; Feringa, B. L. *Nat. Nano.* **2006**, *1*, 25−35.